J|A|C|S COMMUNICATIONS

Published on Web 12/09/2009

Large-Scale Synthesis of SnO_2 Nanosheets with High Lithium Storage Capacity

Cen Wang,[†,‡] Yun Zhou,[‡] Mingyuan Ge,[†,‡] Xiaobin Xu,[†,‡] Zaoli Zhang,[§] and J. Z. Jiang*[,†,‡]

International Center for New-Structured Materials (ICNSM), Zhejiang University, Hangzhou 310027, P.R. China, Department of Materials Science & Engineering, Zhejiang University, Hangzhou 310027, P.R. China, and Erich Schmid Institute of Materials Science, Austrian Academy of Sciences, A-8700 Leoben, Austria

Received November 3, 2009; E-mail: jiangjz@zju.edu.cn

Here, we report a novel SnO_2 nanoarchitecture: extremely thin sheets, with minimum thicknesses of 1.5−3.0 nm. The assemblies of these sheets feature a high Brunauer−Emmett−Teller (BET) surface area and extraordinarily large pore volume, leading to excellent performance in lithium ion batteries.

Owing to its high theoretically gravimetric lithium storage capacity of 782 mAh/g which is more than twice that of the currently commercialized graphite (372 mAh/g) and low potential of lithium ion intercalation, SnO_2 is regarded as one of the most promising candidates for anode materials.[1] It is well established that there are two-step reactions involved in the SnO_2-based working electrode.[2] The first irreversible reaction is responsible for severe capacity loss in the first few cycles which actually results from the formation of electrochemically inactive Li_2O. The second one is reversible with lithium ions repeatedly stored and released between alloying and dealloying processes. However, an intrinsically induced drastic volume change causes a so-called pulverization problem which blocks the electrical contact pathways in the electrode and leads to rapid deterioration in capacity. To enhance the cyclability of the electrode, hybridizing SnO_2 with carbon is effective, but this approach sacrifices the capacity itself due to the introduction of carbon and is usually complicated in fabrication.[3] It is suggested that if single SnO_2 was used as an active material, it should be in a nanometer-sized frame to shorten the pathway lengths of the lithium ion and should possess interior hollow spaces to accommodate large volume change.[4] Herein, we report highly porous SnO_2 nanometer-sized sheets synthesized from a hydrothermal reaction.

In a typical experiment, tin dichloride dihydrate ($SnCl_2 \cdot 2H_2O$, Alfa Aesar, 98%) was added to a basic mixture of ethanol and water (pH ≈ 11) to reach a Sn(II) concentration of 15.8 mM. The obtained white turbid suspension was magnetically stirred for 1 h before being transferred to a Telflon-lined stainless steel autoclave and then heated in an electric oven at 120 °C for 6 h. A yellow product was harvested after centrifugation and dried at 50 °C overnight. The products were characterized by X-ray diffractometer PANalytical X'pert Pro using Cu Kα radiation (λ = 1.5416 Å), transmission electron microscopy (TEM, Philips FEI 200CX operated at 160 kV), high resolution transmission electron microscopy (HRTEM, JEOL 2100F with an image-side C_s-corrector operated at 200 kV), and scanning electron microscopy (SEM, Hitachi S4800 operated at 5 kV). BET surface area and pore volume were tested using Beckman coulter omnisorp100cx. The Li ion battery property was measured by Land CT2001A.

The crystallographic structure of the as-synthesized product is inspected by XRD (Figure S1). All the diffraction peaks can be indexed to a tetragonal rutile-like SnO_2 (cassiterite, Joint Committee on Powder Diffraction Standards (JCPDS) card No. 41-1445, space group: $P4_2/mnm$, a_0 = 4.738 Å, c_0 = 3.1865 Å). No other peaks are detected. Figure 1a displays a typical SEM image of the as-prepared sample. Interestingly, the morphology of the assembled nanosheets reveals a three-dimensional, flower-like appearance. The inherent structure is shown in a TEM image (Figure 1b). In this picture, the light regions suggest planar or bended thin sheets lying on the substrate, with the edge length most likely no more than 100 nm in both dimensions. Dark regions indicate that sheets may either lie aslant, perpendicular to the substrate or spontaneously convolute during the reaction process. The corresponding selected-area electron diffraction (SAED) pattern (inset in Figure 1b) can be indexed as (110), (101), (200), (211), and (301) planes of rutile-type SnO_2 (JCPDS No. 41-1445). Figure 1c shows a C_s-corrected HRTEM image of a planar sheet, in which the atom arrangements are clearly visible along the [1−1−1] projection. Also, this sheet is composed of well-aligned columns except for some defects, i.e. dislocations and twins (marked by blue areas). The insets are two almost identical Fast Fourier Transform (FFT) patterns, corresponding to the respective local areas marked by red dashed lines. One of the patterns is indexed in the bottom right corner with the [1−1−1] zone axis. By means of HRTEM image simulation, the thicknesses at the above two areas from edge to middle are determined to be 1.5−3.0 and 13 nm, respectively. Figure 1d shows a scrolled sheet. Each interplanar spacing is carefully measured at the tip, center, and end of this sheet. Consequently, all three local

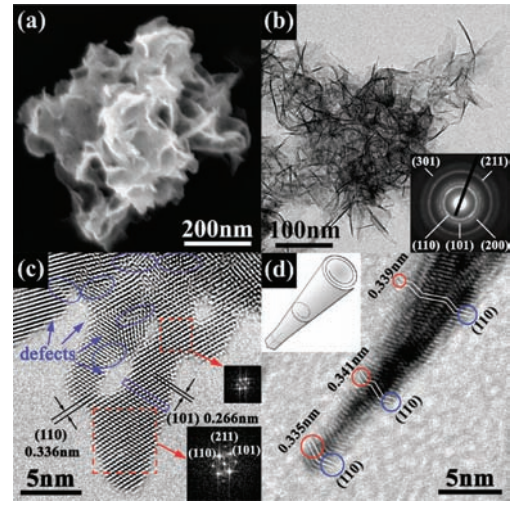

Figure 1. (a) SEM image and (b) TEM image of the as-prepared SnO_2 nanosheets. SAED pattern is shown in the lower right corner of Figure 1b. HRTEM images of (c) a planar SnO_2 sheet and (d) a scrolled SnO_2 sheet with a corresponding model in the upper left inset.

[†] International Center for New-Structured Materials (ICNSM), Zhejiang University.
[‡] Department of Materials Science & Engineering, Zhejiang University.
[§] Austrian Academy of Sciences.

10.1021/ja909321d

crystal planes turn out to belong to the same (110) plane. On the fringes, the lattices of these zones at one side (marked by red circles) are orientated to the same direction, and coincidently, it is the same at the opposite side (marked by blue circles). In addition, the contrasts at the turning points of each quasi-twinned lattice vary sharply, forming the 2-, 4-, and 6-fold areas. All these phenomena strongly support the scrolled nature of this sort of structure which can be ascribed to the minimization of surface energy. A model is illustrated in the inset of Figure 1d.

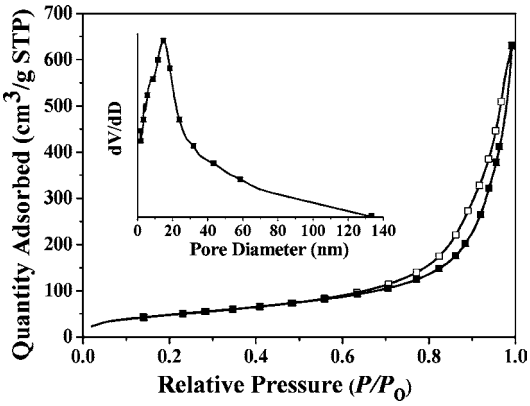

Figure 2. Nitrogen adsorption and desorption isotherms of SnO_2 nanosheets shown in Figure 1 at 77 K with corresponding pore-size distribution (inset) calculated by BJH method from desorption branch.

The product is further characterized by nitrogen adsorption and desorption isotherms at 77 K and corresponding pore size distribution (inset) in Figure 2. It is found that the overall SnO_2 nanosheets have a BET surface area of 180.3 m^2/g with an average Barretl−Joyner−Halenda (BJH) pore diameter of 16.2 nm and a pore volume of 1.028 cm^3/g. To our knowledge, this high value of pore volume has never been achieved in pure SnO_2 crystallites.[5] The isotherm is characteristic of a type IV with a type H3 hysteresis loop, revealing that the material is composed of aggregates (loose assemblages) of sheet-like particles forming slit-like pores, in correspondence with our microscopy findings.[6]

Motivated by the unique inherent structure of SnO_2 product prepared here, we performed lithium storage tests as an anode material (see Supporting Information for experimental details). The cell was charged and discharged at a constant current of 0.1 C (78.2 mA/g) and a fixed voltage window between 3 V and 5 mV. Three plateaus are present at approximately 0.9, 0.6, and 0.3 V in the first discharge curve and might be respectively ascribed to the formation of the solid electrolyte interface (SEI), Li_2O and Li_xSn ($0 \le x \le 4.4$) alloy (Figure S2). In Figure 3, it can be easily found that our material exhibits a high discharge capacity of 559 mAh/g after 20 cycles with the retention of 57%. Also, the Coulombic efficiency keeps steadily more than 95%. Recently, Park et al. reported a SnO_2/graphene hybridization, which also exhibited enhanced cyclic performance.[7] The introduction of graphene plays dual roles; i.e., it increases the electrode conductivity and acts as a buffer layer to contain stresses induced by volume change. In comparison, the charge capacity of SnO_2/graphene remains ~593 mAh/g after 20 cycles which is slightly higher than our results of 559 mAh/g. Nevertheless, considering we applied a wider cutoff window and larger constant current which are prone to create relatively harsher destruction and resistance of the electrode, the material reported here is very attractive due to its facile, economical, and high purity synthesis.[8] Its performance via hybridization will be further studied.

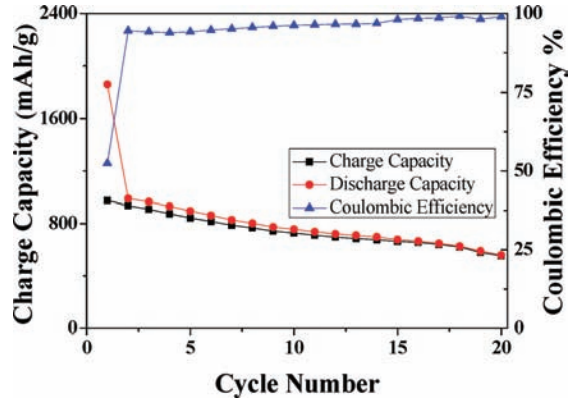

Figure 3. Charge and discharge capacities as well as Coulombic efficiency as a function of cycle number with SnO_2 electrode in button cell.

In summary, extremely thin SnO_2 nanosheets were successfully synthesized through a facile one-pot hydrothermal method. The as-prepared products possess a surprisingly high BET surface area and pore volume and exhibit a superior lithium storage capacity and cycle performance as an anode in lithium-ion batteries. The inherent characteristics of this nanostructure may also open up prospects for gas sensors or photocatalysis devices.

Acknowledgment. Financial support from the National Natural Science Foundation of China (Grant Nos. 60776014, 60876002 and 50920105101), Zhejiang University-Helmholtz cooperation fund, the Ministry of Education of China (Program for Changjiang Scholars), the Department of Science and Technology of Zhejiang province, and the BaoYuGang foundation of Zhejiang University is gratefully acknowledged.

Supporting Information Available: The XRD pattern and first cycle performance (Figures S1 and S2) as well as experimental details. This material is available free of charge via the Internet at http://pubs.acs.org.

References

(1) (a) Wang, Y.; Zeng, H. C.; Lee, J. Y. *Adv. Mater.* **2006**, *18*, 645–649. (b) Park, M. S.; Wang, G. X.; Kang, Y. M.; Wexler, D.; Dou, S. X.; Liu, H. K. *Angew. Chem., Int. Ed.* **2007**, *46*, 750–753. (c) Demir-Cakan, R.; Hu, Y. S.; Antonietti, M.; Maier, J.; Titirici, M. M. *Chem. Mater.* **2008**, *20*, 1227–1229. (d) Lou, X. W.; Li, C. M.; Archer, L. A. *Adv. Mater.* **2009**, *21*, 2536–2539.

(2) (a) Courtney, I. A.; Dahn, J. R. *J. Electrochem. Soc.* **1997**, *144*, 2045–2052. (b) Brousse, T.; Retoux, R.; Herterich, U.; Schleich, D. M. *J. Electrochem. Soc.* **1998**, *145*, 1–4. (c) Courtney, I. A.; McKinnon, W. R.; Dahn, J. R. *J. Electrochem. Soc.* **1999**, *146*, 59–68.

(3) (a) Sun, X. M.; Liu, J. F.; Li, Y. D. *Chem. Mater.* **2006**, *18*, 3486–3494. (b) Wen, Z. H.; Wang, Q.; Zhang, Q.; Li, J. H. *Adv. Funct. Mater.* **2007**, *17*, 2772–2778. (c) Chen, G.; Wang, Z. Y.; Xia, D. G. *Chem. Mater.* **2008**, *20*, 6951–6956. (d) Chen, J. S.; Cheah, Y. L.; Chen, Y. T.; Jayaprakash, N.; Madhavi, S.; Yang, Y. H.; Lou, X. W. *J. Phys. Chem. C* **2009**, *113*, 20504–20508.

(4) (a) Kim, C.; Noh, M.; Choi, M.; Cho, J.; Park, B. *Chem. Mater.* **2005**, *17*, 3297–3301. (b) Wang, Y.; Lee, J. Y.; Zeng, H. C. *Chem. Mater.* **2005**, *17*, 3899–3903. (c) Lou, X. W.; Wang, Y.; Yuan, C. L.; Lee, J. Y.; Archer, L. A. *Adv. Mater.* **2006**, *18*, 2325–2329.

(5) (a) Ba, J. H.; Polleux, J.; Antonietti, M.; Niederberger, M. *Adv. Mater.* **2005**, *17*, 2509–2512. (b) Yang, H. X.; Qian, J. F.; Chen, Z. X.; Ai, X. P.; Cao, Y. L. *J. Phys. Chem. C* **2007**, *111*, 14067–14071. (c) Chandra, D.; Mukherjee, N.; Mondal, A.; Bhaumik, A. *J. Phys. Chem. C* **2008**, *112*, 8668–8674.

(6) Kruk, M.; Jaroniec, M. *Chem. Mater.* **2001**, *13*, 3169–3183.

(7) Paek, S. M.; Yoo, E.; Honma, I. *Nano Lett.* **2009**, *9*, 72–75.

(8) Kim, M. G.; Cho, J. *Adv. Funct. Mater.* **2009**, *19*, 1497–1514.

JA909321D